Structures and phase transitions of $PrBGeO_5$ in the temperature range $20\text{-}800\,^{\circ}C$

1998 J. Phys.: Condens. Matter 10 9975

(http://iopscience.iop.org/0953-8984/10/44/006)

J. Phys.: Condens. Matter **10** (1998) 9975–9989. Printed in the UK PII: S0953-8984(98)92660-1

Structures and phase transitions of $PrBGeO_5$ in the temperature range 20–800 °C

E L Belokoneva†, W I F David‡, J B Forsyth‡§ and K S Knight‡

† Moscow State University, 119899 Moscow, Russia

‡ Rutherford Appleton Laboratory, Chilton, Oxfordshire OX11 0QX, UK

Received 17 March 1998, in final form 16 June 1998

Abstract. High-resolution neutron powder diffractometry has been used to characterize the structural phase transitions which occur in $PrBGeO_5$ at 550 and 750 °C. The change in lattice parameters of the trigonal unit cell as a function of temperature, observed in the range from ambient to 800 °C, shows that the 550 °C transition is associated with an abrupt contraction of the unit cell volume. The crystal structure stable in the temperature interval between 550 and 750 °C is isomorphous with the stillwellite structure of $LaBGeO_5$ in its polar variant stable up to 530 °C. The phase transition at 750 °C to a non-polar variant of the structure mimics the 530 °C transition in $LaBGeO_5$. The structural parameters of these two $PrBGeO_5$ phases have been refined from data taken at 650, 770 and 800 °C. The structure of the $PrBGeO_5$ phase stable at ambient temperature gives rise to extra reflections not given by the stillwellite structure. These can be indexed on a triple cell with $a' \approx \sqrt{3}a$, $c' \approx c$ and the structure has been determined and refined from a combination of neutron powder data and an ambient temperature single crystal x-ray diffraction study.

1. Introduction

Perfect single crystals of $LaBGeO_5$, an analogue of the mineral stillwellite (Ce,La)$BSiO_5$, were produced recently by the Czochralski technique [1]. This crystal possesses many physical properties (ferroelectric [2], non-linear optic [2, 3] and laser [1, 4]) which may find device applications and which have stimulated interest in enlarging the stillwellite family of compounds. A number of isomorphs $RBGeO_5$, where R = La ... Er, Y, have been synthesized by Mill [1]. The crystal structure of the mineral stillwellite (Ce,La)$BSiO_5$ is acentric and polar. The room temperature polar structure of its $LaBGeO_5$ isomorph has been determined using single crystal x-ray methods [1, 5] and is shown in figure 1. A polymorphic transition occurs at Nd in the rare earth series, the more stable structure of $NdBGeO_5$ being that of datolite, $CaBSiO_4(OH)$, which is centrosymmetric, though both modifications occur. This polymorphic transition is related to the decrease in the ionic radius of R with increasing atomic number.

A ferroelectric phase transition in $LaBGeO_5$ at 530 °C was established by different methods [2, 6, 7]. In a recent study [8] using the high-resolution powder diffractometer (HRPD) at the pulsed neutron source ISIS, the pseudo symmetry in the stillwellite structure [9] was used as a basis for describing the phase transition from the polar structure in space group $P3_1$ to the high temperature, non-polar phase in $P3_121$ and developing a high-temperature model. That phase transition is of second order, but contains both displacive

§ Now at the Clarendon Laboratory, University of Oxford, South Parks Road, Oxford OX1 3PU, UK.

0953-8984/98/449975+15$19.50

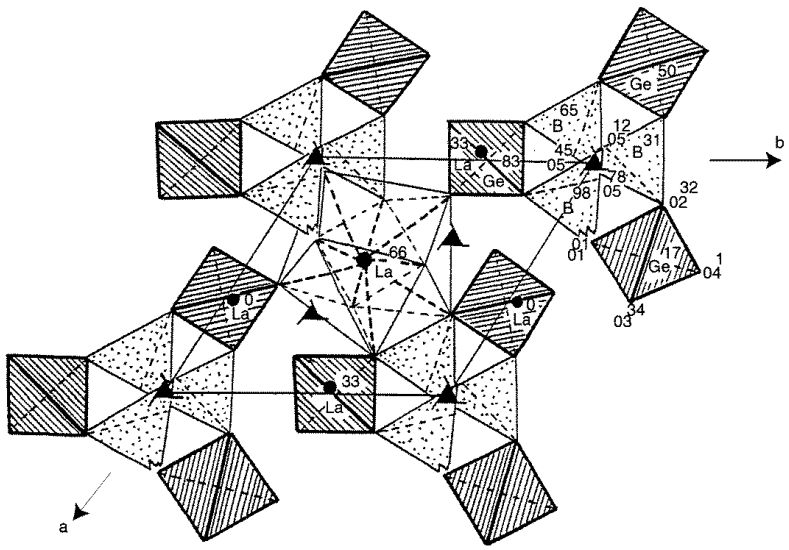

Figure 1. The [001] projection of the polar stillwellite structure of $LaBGeO_5$ at ambient temperature [8]. The figures indicate the heights of the atoms in hundredths of the *c* dimension.

and order-disorder components in accordance with the results of the physical measurements described above.

We now report similar investigations of the related phase $PrBGeO_5$ which was also believed to have the stillwellite structure at room temperature. Single crystals of this new member of the stillwellite family were also grown by Mill using the Czochralski method. In contrast to $LaBGeO_5$, two-phase transitions were detected by Stefanovich [10] both in the temperature dependence of dielectric susceptibility and dielectric loss in single crystals and also in second-harmonic generation, (SHG), in powdered samples. The lower temperature transition occurs at 537 °C on heating and 497 °C on cooling and is of first order. The higher temperature transition at 742 °C is ferroelectric, second order and is analogous to the transition in $LaBGeO_5$ at 530 °C. A remarkable feature of the temperature dependence of the SHG intensity is that it increases sharply with increasing temperature at 537 °C as shown in figure 2. It has also been found [11] that a small addition of La into $PrBGeO_5$ reduces this jump in the SHG signal and finally, at $(Pr_{0.8}La_{0.2})BGeO_5$, this signature of the phase transition disappears.

2. Experimental

The first attempt to determine the crystal structure of $PrBGeO_5$ at room temperature was made, as it was for $LaBGeO_5$, using single crystal x-ray diffraction data. Laue photographs of most crystals gave evidence of twinning. The intensities from the best spherical sample ($r = 0.1$ mm) were measured within a complete hemisphere and then averaged, save for the Friedel pairs, to give 2827 independent reflections. The refinement of a model identical to that for $LaBGeO_5$ at room temperature converged to $R_{hkl} \sim 4\%$. Analysis of the atomic coordinates and anisotropic thermal vibration parameters showed that the pseudosymmetry is more pronounced in $PrBGeO_5$ than in $LaBGeO_5$. We can conclude that, within the standard deviations, Pr and Ge atoms occupy special positions on two-fold axes and that

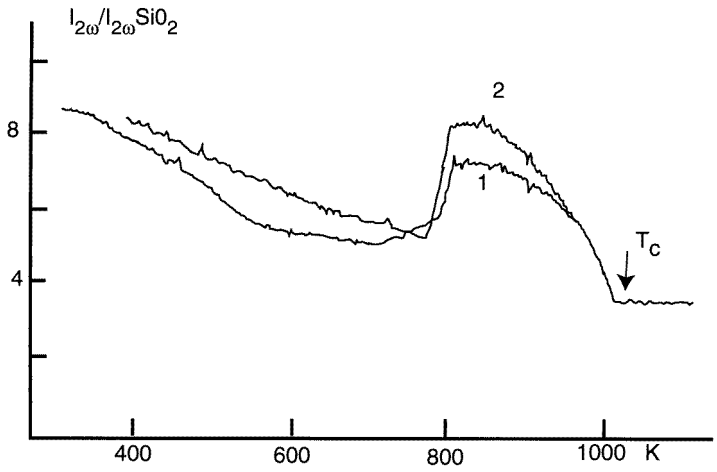

Figure 2. The temperature dependence of the ratio of intensity of second-harmonic generation (SHG) in $PrBGeO_5$ during heating (1) and cooling (2) compared to that in silica [10].

two pairs of oxygens O(1)–O(2) and O(3)–O(4) are connected by two-fold axes. The anisotropic temperature parameters of boron, and especially O(5) atoms, were significantly increased. The residual electron density, $\Delta\rho$, map calculated using the atomic coordinates of Pr, Ge, O(1)–O(4), gave four peaks of equal height, which correspond to two pairs of positions for O(5), O(5′) and B, B′, connected by two-fold axes. A model with split sites for O(5) and B improved the refinement, $R_{hkl} = 3\%$, but such a model cannot be correct since it corresponds to the non-polar space group $P3_121$ whereas the structure at room temperature is certainly polar. Thus, the room temperature structure of $PrBGeO_5$ could not be determined completely from the x-ray data.

In view of our previous successful experience with the neutron powder diffraction study of $LaBGeO_5$, we have now undertaken an investigation of powdered $PrBGeO_5$ over a wide temperature interval from room temperature to 1073 K using HRPD. The specimen was prepared by crushing and grinding single crystal material containing, as we now know, boron enriched to 99(1)% in the low-absorbing isotope ^{11}B. Some 14.8 g of the powder with particle size less than 150 μm were sealed in a Ti/Zr null matrix can with thin vanadium windows and a rectangular cross section $40 \times 23 \times 3$ mm. This container was oriented in a furnace on HRPD so that the minor dimension of the can was parallel to the incident neutron beam and the major dimension was vertical. This geometry was chosen to optimize the diffracted intensity into the backward-angle bank of detectors from what was believed at first to be a highly absorbing specimen. Vanadium was also used as the material for the furnace windows and resistance heating elements to reduce their contribution to the features of the diffraction patterns at the expense of an increase in the incoherent background. Time of flight data were collected in the range 30–130 ms at 5 Hz repetition rate, normalized using the spectra from the main beam monitor and corrected for the wavelength dependence of the detector, the empty sample container and the specimen absorption. The data sets used in the Rietveld refinements extended from 35–115 ms, corresponding to a range of d-spacing between 0.7 and 2.3 Å. Two series of short runs of approximately 30 min duration (total incident proton beam current 12 μA h) provided patterns which could be refined to give unit cell dimensions accurate to parts in 10^5 and were used to follow the temperature dependence of the lattice parameters below and above the two transition temperatures and

clearly establish the changes in unit cell volume to be associated with the three different phases. Longer runs for accurate structure refinements at 20, 100, 650, 770 and 800 °C were accumulated for 563, 150, 170, 150 and 257 μA h, respectively, and the 20 °C data set was augmented by a second data set measured for 207 μA h covering the range 100–200 ms which extends the d-spacing range to 3.9 Å. Structural analysis was performed using the Rietveld method with program TF12 based on the Cambridge Crystallography Subroutine Library (CCSL).

The profile of the 150 μA h^{-1} data set at 100 °C revealed extra lines which could be indexed on a triple cell with $a' \approx \sqrt{3}a$, $c' \approx c$ (denoted H3$_1$) relative to the stillwellite cell dimensions of $a = 6.941$ Å and $c = 6.898$ Å. This was subsequently confirmed when the 20 °C data sets had been analysed.

3. The temperature variation of the unit cell dimensions from ambient to 800 °C

Figure 3 illustrates the behaviour of the unit cell dimensions and the cell volume of $PrBGeO_5$ as a function of temperature. The dimensions of the unit cell are smaller than those of $LaBGeO_5$. With increasing temperature c dimensions increase, and a dimensions decrease, in both materials. However, in contrast to $LaBGeO_5$ where the changes in c and a dimensions are continuous, in $PrBGeO_5$ the c dimension increases discontinuously with an 0.020 Å jump from ∼6.845 to ∼6.858 Å at the lower, 547 °C, transition point, whereas the a axis decreases by 0.008 Å, also with a sharp jump, from 6.951 to 6.943 Å in the same temperature (table 1). The presence of a small continuous component may be connected with the presence of defects in the crystals. The unit cell volume, V, reduces by ∼0.07(1) Å^3 from 286.35 to 286.28 Å^3 on heating through the transition. The a, c and V values in figure 3 are normalized to emphasize the discontinuity in this weak first-order phase transition in contrast to the continuous second-order phase transition in $LaBGeO_5$ at 530 °C. The phase transition which occurs in $PrBGeO_5$ at 742 °C is similar to that in $LaBGeO_5$ at 530 °C: there is no change in the slope of the volume-temperature curve illustrated to the right-hand side of figure 3(c) and the dimension of the c axis increases monotonically in the second-phase transition, whereas the dimension of the a axis decreases (figures 3(a) and (b)).

The first-order phase transition at 547(1) °C is between phases having the same polar symmetry $P3_1$, but different unit cells. The parameters of the ambient temperature crystal structure have been refined from the long run taken at 20 °C. The transition at 750 °C mimics the transition in $LaBGeO_5$ and is between the polar $P3_1$ and non-polar $P3_12_1$ structures which have been refined from long runs taken at 650 °C for the former and at 800 °C for the latter structure.

The a/c ratio is a sensitive characteristic of the ferroelectric phase transition in the stillwillite structure type and has a value ∼1.007–1.006 for paraelectric phases. In $LaBGeO_5$ the a/c ratio changes from 1.0206 at room temperature through 1.0097 (525 °C) and 1.0088 (535 °C) to 1.0073 for the high-temperature phase (at 630 °C). The phase transition in the isomorphous phase $LaBSiO_5$, $T_c = 140$ °C [12, 13], is characterized by a change in the a/c ratio from 1.0096 at room temperature to 1.0071 in the paraelectric phase at 200 °C. In $PrBGeO_5$ the a/c ratio changes from 1.0206 at room temperature to 1.0109 at 650 °C for the intermediate but still polar phase and then to 1.0062 in the high-temperature modification at 800 °C.

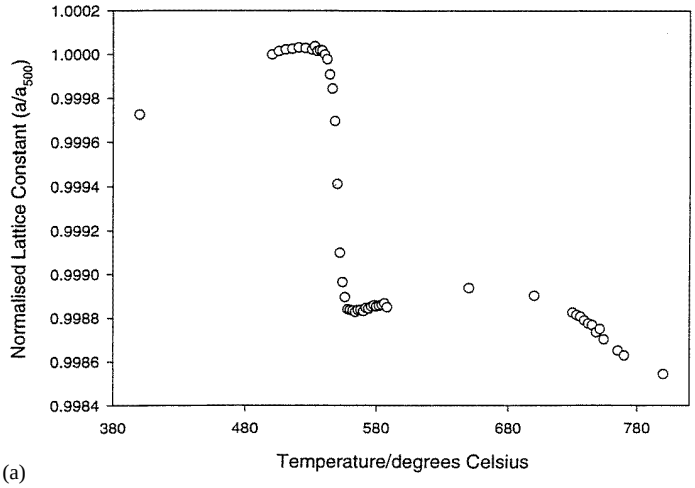

(a)

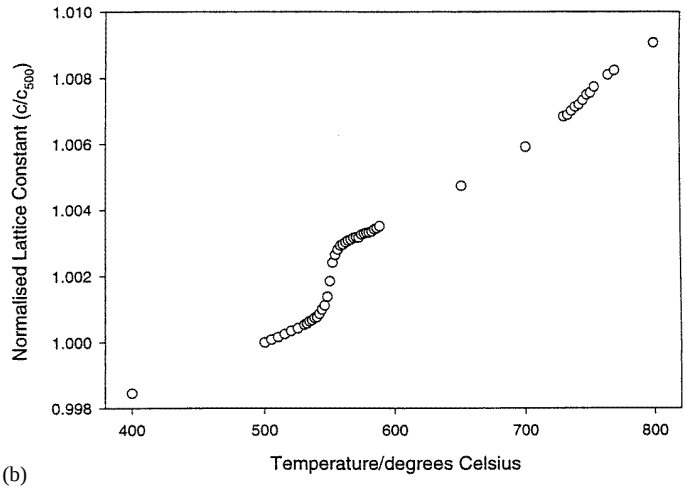

(b)

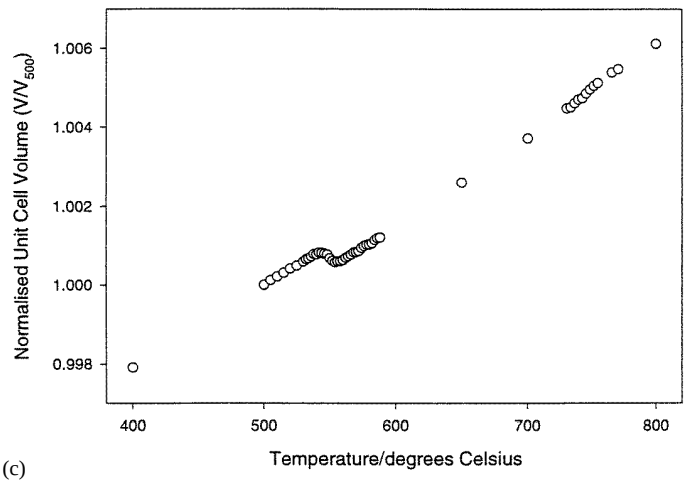

(c)

Figure 3. The temperature variation of the trigonal unit cell dimensions of $PrBGeO_5$ (a) *a*, (b) *c* and (c) the volume, normalized to values at 500 °C.

Table 1. The temperature variation of the lattice parameters and unit cell volume of $PrBGeO_5$. The estimated standard deviations are (1), (2) and (1) in the least significant figures quoted, respectively.

T(°C)	a(Å)	c (Å)	V(Å^3)	T(°C)	a(Å)	c (Å)	V(Å^3)
20	12.0202	6.7999	283.62 × 3	566	6.9430	6.8589	286.34
400	6.9499	6.8367	285.63	568	6.9430	6.8593	286.35
500	6.9511	6.8376	286.12	570	6.9430	6.8594	286.35
505	6.9511	6.8383	286.15	572	6.9431	6.8593	286.36
510	6.9512	6.8388	286.18	574	6.9430	6.8599	286.39
515	6.9513	6.8394	286.20	576	6.9431	6.8601	286.40
520	6.9513	6.8400	286.23	578	6.9432	6.8603	286.41
525	6.9513	6.8406	286.26	580	6.9431	6.8604	286.41
530	6.9512	6.8414	286.28	582	6.9431	6.8606	286.42
532	6.9513	6.8416	286.30	584	6.9432	6.8611	286.44
534	6.9512	6.8420	286.31	586	6.9432	6.8613	286.46
536	6.9512	6.8423	286.32	588	6.9431	6.8617	286.46
538	6.9512	6.8428	286.34	650	6.9436	6.8688	286.80
540	6.9511	6.8429	286.34	700	6.9442	6.8778	287.22
542	6.9509	6.8436	286.35	730	6.9436	6.8840	287.44
544	6.9504	6.8445	286.35	733	6.9436	6.8844	287.45
546	6.9500	6.8452	286.34	736	6.9435	6.8852	287.478
548	6.9490	6.8471	286.34	739	6.9434	6.8861	287.50
550	6.9470	6.8503	286.31	742	6.9433	6.8865	287.51
552	6.9448	6.8541	286.29	745	6.9432	6.8874	287.55
554	6.9439	6.8558	286.28	748	6.9430	6.8886	287.58
556	6.9434	6.8568	286.29	751	6.9431	6.8890	287.60
558	6.9430	6.8577	286.29	754	6.9428	6.8902	287.62
560	6.9430	6.8579	286.30	765	6.9424	6.8927	287.70
562	6.9430	6.8584	286.31	770	6.9423	6.8936	287.72
564	6.9429	6.8587	286.32	800	6.9408	6.8983	287.80

4. The structure of the ambient temperature phase of $PrBGeO_5$

Having observed the tripling of the unit cell in the neutron powder profile, we returned to the x-ray diffraction experiment using the same single crystal but the tripled unit cell. Additional reflections corresponding to the enlarged cell were found, but these were weak and only 22 had intensities which were statistically significant, in number less than 1% of fundamental reflections. The structure of the phase stable at ambient temperature has then been determined from the neutron powder data starting from the knowledge that extra reflections due to the triple cell are very weak in the single crystal x-ray diffraction experiment.

The positional parameters for Pr and Ge in a model for the triple unit cell must remain close to those for the structure found for the average small unit cell from the x-ray data set. They are close to special positions on two-fold axes and two pairs of oxygens are almost related by two-fold axes. The tripling and polarity can only result from a different distribution of O(5) and B atoms, whose electron density could not be best modelled by a polar structure within the small (averaged) unit cell. Between the two positions for O(5) and B determined in $\Delta\rho$, we can distinguish two orientations: left and right, or 'black' and 'white' (figure 4(a)). The unit cell will be tripled if these atoms occupy different orientations, for example, two 'black' and one 'white' around the three-fold axes, and the structure will be polar. In the new enlarged unit cell (figure 4(b)) we have 3 Pr, 3 Ge,

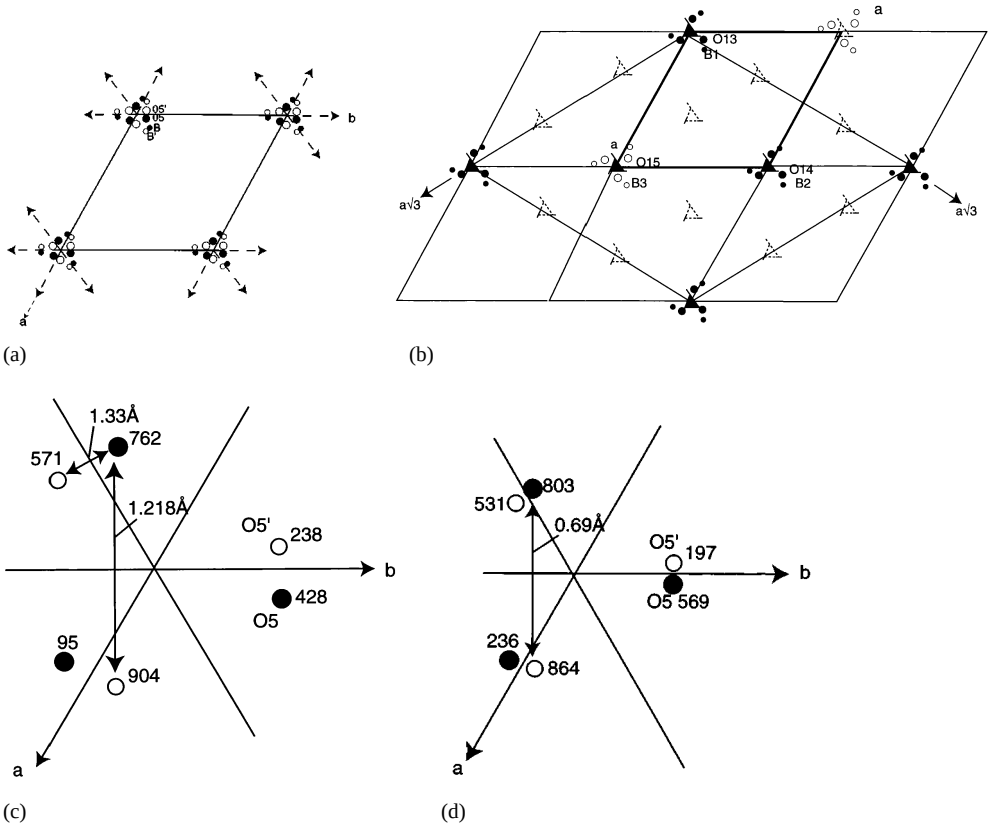

Figure 4. (a) Two (black and white) positions of O(5) and B in the small (average) unit cell, (b) tripled unit cell with $a_{new} = \sqrt{3}a$ and its connection with the small unit cell, a, in room temperature modification of $PrBGeO_5$. Different orientations of O(13), O(14) (black) and O(15) (white) atoms and B(1), B(2) (black) and B(3) (white) atoms are shown around the three three-fold axes; the pseudosymmetric elements are shown by broken lines. (c) and (d) see text.

15 O and 3 B independent atoms but the peculiarities of the new model are determined principally by only one O(15) oxygen and one B(3) atom in the same space group $P3_1$. This model implies that the major contribution to additional reflections will originate from the elements oxygen and boron and explains why the additional reflections and tripling of the unit cell were missed in the original x-ray experiment but found in the neutron pattern from HRPD.

The model for the tripled cell corresponds to space group $P3_1$. The pseudosymmetry is high corresponding to $P3_112$ ($P3_121$ in the small unit cell) since the three Pr and the three Ge atoms occupy positions which are close to being special, $(x, 2x)$, on the diagonal diads. The oxygens O1–O12 are connected in pairs by the two-fold axis and only three oxygens, O13, 14, 15 and three borons, B1, 2, 3 break this rule, as is illustrated in figure 4(b) which also shows that there are several pseudo-three-fold axes in the tripled unit cell. The presence of such pseudosymmetry complicates the structure refinement since it leads to high correlations between the atomic positional parameters. Such crystals must have a strong tendency to domain formation and twinning, and that is observed in x-ray Laue photographs of $PrBGeO_5$ taken at ambient temperature (see the introduction).

Refinements of the tripled unit cell model were carried out with both x-ray and neutron data. The sense of the a^* and b^* axes in $P3_1$ cannot be determined in the x-ray diffraction experiment, so in accordance with our choice we must use the $-x$, $-y$, z setting to compare with the $LaBGeO_5$ parameters for the small (average) unit cell. The initial atomic coordinates from the average unit cell for $PrBGeO_5$ were transformed to the new, enlarged $\sqrt{3}a$ cell and refined. The atomic coordinates x, y and z of O(13)('black'), O(14)('black'), O(15)('white'), B(1)('black'), B(2)('black') and B(3)('white') were fixed because of the high correlation. The refinement of the x-ray diffraction data including isotropic temperature parameters for all atoms gave $R_{hkl} = 3.81\%$ and $R_{whkl} = 3.82\%$ for 2849 reflections (table 2).

The model with fully ordered sites for oxygen and boron atoms in the triple cell was also used as the starting point for refinement of the neutron data collected in the long runs. The atomic coordinates of the high atomic number Pr and Ge atoms determined from the x-ray data were initially fixed in the neutron refinements. The positional parameters of all oxygen and boron atoms were then adjusted in a constrained refinement which required equality of all B–O and all Ge–O bonds to within 0.05 Å. Reasonable isotropic temperature factors were fixed for all atoms: 0.5, 0.4, 0.8 and 0.8 $Å^{-2}$ for Pr, Ge, O and B atoms, respectively. The positional parameters for Pr and Ge were included in the last three cycles of refinement without significant change. The resulting profile agreement factor was $R_{prof} = 7.16\%$, $R_{wprof} = 6.33\%$ and $\chi^2 = 5.937$ for 5957 observations, figure 5, table 2. The interatomic distances correspond to the accepted values (table 3).

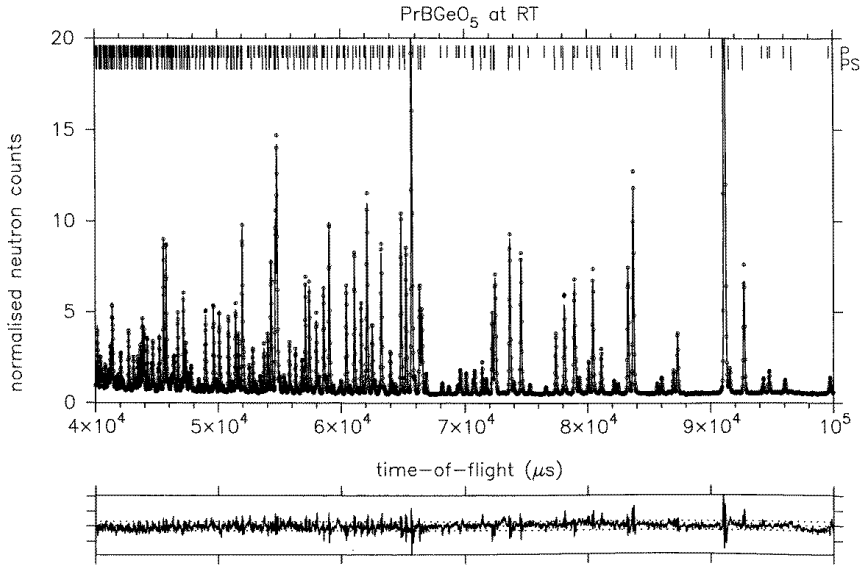

Figure 5. Powder profile refinements of $PrBGeO_5$ of the low-temperature phase using data taken at 20 °C. The calculated positions of reflections from the small and tripled unit cell are shown by the lower and upper sets of markers, respectively. The difference between observed and calculated profiles divided by the estimated standard deviation (esd) of the observed is plotted in the lower pattern of each profile figure here and in figures 6 and 7; horizontal broken lines are drawn at ±1 and ±3 esd.

Table 2. The positional and thermal parameters of the ambient temperature phase of $PrBGeO_5$ as determined at 20 °C from x-ray single crystal and neutron HRPD data.

Atom	x	y	z	B_j
X-ray, 20 °C				
Pr(1)	0.2763(3)	0.1378(3)	0	0.49(2)
Pr(2)	0.5284(3)	0.4710(3)	0.3363(5)	0.45(2)
Pr(3)	0.1959(3)	0.3914(3)	0.6620(5)	0.43(2)
Ge(1)	0.2805(5)	0.1386(5)	0.5004(9)	0.43(2)
Ge(2)	0.5268(5)	0.4744(5)	0.8338(8)	0.41(2)
Ge(3)	0.1948(6)	0.3866(6)	0.1632(7)	0.40(3)
O(1)	0.653(3)	0.496(3)	−0.327(3)	0.58(3)
O(2)	0.822(2)	0.810(2)	0.010(3)	0.91(3)
O(3)	0.504(3)	0.684(3)	0.340(3)	0.59(3)
O(4)	0.172(3)	0.155(2)	−0.340(3)	0.94(3)
O(5)	0.506(3)	0.351(3)	−0.007(4)	0.89(3)
O(6)	0.326(3)	0.482(3)	0.319(3)	0.93(3)
O(7)	0.561(3)	0.590(3)	0.007(3)	0.99(3)
O(8)	0.748(2)	0.635(2)	−0.655(3)	1.02(3)
O(9)	0.683(2)	0.759(2)	0.677(3)	1.03(3)
O(10)	0.221(2)	0.302(2)	−0.017(3)	1.03(3)
O(11)	0.356(2)	0.260(1)	0.326(2)	1.00(3)
O(12)	0.416(3)	0.438(3)	0.660(4)	1.03(3)
O(13)	−0.0303	−0.0373	0.7650	0.53(3)
O(14)	0.3265	0.6293	0.5660	0.67(3)
O(15)	0.6598	0.2960	0.5660	0.67(3)
B(1)	0.0710	−0.0419	0.9720	0.58(3)
B(2)	0.2629	0.6380	1.0300	0.63(3)
B(3)	0.5962	0.3047	1.0300	0.63(3)
Neutron HRPD, 20 °C				ITF
Pr(1)	0.2766	0.1400	0	0.56
Pr(2)	0.5289	0.4708	0.3287	0.56
Pr(3)	0.1935	0.3906	0.6627	0.56
Ge(1)	0.2817	0.1390	0.5000	0.73
Ge(2)	0.5251	0.4711	0.8243	0.73
Ge(3)	0.1921	0.3867	0.1617	0.73
O(1)	0.6774(7)	0.4884(7)	0.6604(14)	0.90
O(2)	0.8299(8)	0.8174(8)	0.0109(13)	0.90
O(3)	0.5143(6)	0.6783(8)	0.3295(14)	0.90
O(4)	0.1697(6)	0.1518(6)	0.6496(11)	0.90
O(5)	0.4936(8)	0.3436(8)	0.9858(14)	0.90
O(6)	0.3184(6)	0.4956(7)	0.3156(15)	0.90
O(7)	0.5599(8)	0.5880(9)	0.0016(11)	0.90
O(8)	0.7497(8)	0.6301(7)	0.3389(11)	0.90
O(9)	0.6934(9)	0.7732(8)	0.6639(12)	0.90
O(10)	0.2386(6)	0.3149(7)	−0.0193(11)	0.90
O(11)	0.3490(8)	0.2591(9)	0.3178(13)	0.90
O(12)	0.4077(8)	0.4387(8)	0.6444(13)	0.90
O(13)	−0.0287(7)	−0.0376(5)	0.7709(10)	0.90
O(14)	0.3048(7)	0.6302(6)	0.7619(11)	0.90
O(15)	0.6606(7)	0.2960(7)	0.5711(9)	0.90
B(1)	−0.0710(7)	−0.0454(6)	0.9713(12)	0.51
B(2)	0.2621(7)	0.6229(6)	0.9612(12)	0.51
B(3)	0.5930(8)	0.3022(7)	1.0301(11)	0.51

Table 3. The temperature variation of cation–oxygen interatomic distances (in Å) in the Pr-polyhedron and B- and Ge-tetrahedra.

20 °C		
Pr(1)-polyhedron	Pr(2)-polyhedron	Pr(3)-polyhedron
O(1)–2.718	O(1)–2.619	O(2)–2.570
O(2)–2.715	O(3)–2.586	O(3)–2.642
O(4)–2.744	O(5)–2.703	O(4)–2.740
O(5)–2.534	O(6)–2.694	O(6)–2.743
O(8)–2.561	O(7)–2.558	O(7)–2.343
O(9)–2.399	O(8)–2.374	O(9)–2.571
O(10)–2.368	O(11)–2.378	O(10)–2.508
O(11)–2.496	O(12)–2.514	O(12)–2.343
O(13)–2.591	O(16)–2.557	O(15)–2.586
B(1)-tetrahedron	B(2)-tetrahedron	B(3)-tetrahedron
O(2)–1.498	O(3)–1.490	O(1)–1.515
O(4)–1.506	O(6)–1.510	O(5)–1.536
O(13)–1.441	O(15)–1.437	O(16)–1.440
O(13′)–1.447	O(15′)–1.445	O(16′)–1.492
Si(1)-tetrahedron	Si(2)-tetrahedron	Si(3)-tetrahedron
O(2)–1.746	O(1)–1.773	O(3)–1.788
O(4)–1.753	O(5)–1.766	O(6)–1.768
O(8)–1.671	O(7)–1.737	O(9)–1.664
O(11)–1.763	O(12)–1.758	O(10)–1.747
650 °C		
Pr-polyhedron	B-tetrahedron	Si-tetrahedron
O(3)–2.574	O(1)–1.523	O(1)–1.739
O(3′)–2.369	O(2)–1.511	O(2)–1.778
O(4)–2.399	O(5)–1.450	O(3)–1.707
O(4′)–2.540	O(5′)–1.462	O(4)–1.705
O(1)–2.616		
O(1′)–2.783		
O(2)–2.712		
O(2′)–2.660		
O(5)–2.639		
800 °C		
Pr-polyhedron	B-tetrahedron	Si-tetrahedron
O(1) × 2–2.754	O(1) × 2–1.514	O(1) × 2–1.747
O(1′) × 2–2.644	O(5) × 2–1.578	O(3) × 2–1.711
O(3) × 2–2.563		
O(3′) × 2–2.373		
O(5) × 2–2.688	O(5)–O(5′)–0.746	

5. The structure of the intermediate and higher temperature phases of $PrBGeO_5$

The structure of the intermediate phase was refined using data from the long run collected at 650 °C. The atomic coordinates obtained earlier [5, 8] for the low-temperature setting and the normal (small) unit cell of stillwellite were used as initial parameters. The coordinate transformation from the low-temperature setting to the high-temperature setting is $x_H = x_L -$

y_L, $y_H = x_L$, $z_H = z_L$, and back from the high-temperature setting to the low-temperature setting is $x_L = y_H$, $y_L = -x_H + y_H$, $z_L = z_H$. Both the thermal vibrational parameters (table 4) and the interatomic distances obtained from the refinement have normal values (table 3). The resulting profile agreement factor was $R_{prof} = 5.45\%$, $R_{wprof} = 6.08\%$ and $\chi^2 = 1.667$ for 2503 observations, figure 6. The structure is similar to that of $LaBGeO_5$ at room temperature.

Table 4. The positional and thermal parameters of the intermediate-temperature phase of $PrBGeO_5$ as determined at 650 °C from neutron HRPD data.

Atom	*x*	*y*	*z*	ITF
Pr	0.5879(18)	0.0001(32)	0	1.12(8)
Ge	0.5761(9)	−0.0014(17)	0.4982(26)	1.05(6)
B	0.1107(14)	0.0048(23)	0.9757(21)	0.84(9)
O(1)	0.3457(20)	0.1913(20)	0.0200(24)	1.64(19)
O(2)	0.1919(17)	0.3388(18)	0.3242(26)	1.37(18)
O(3)	0.6193(17)	0.4852(18)	0.3401(25)	1.62(16)
O(4)	0.4432(17)	0.6060(19)	−0.0116(28)	2.55(22)
O(5)	0.0542(11)	0.0456(12)	0.7827(23)	1.40(10)

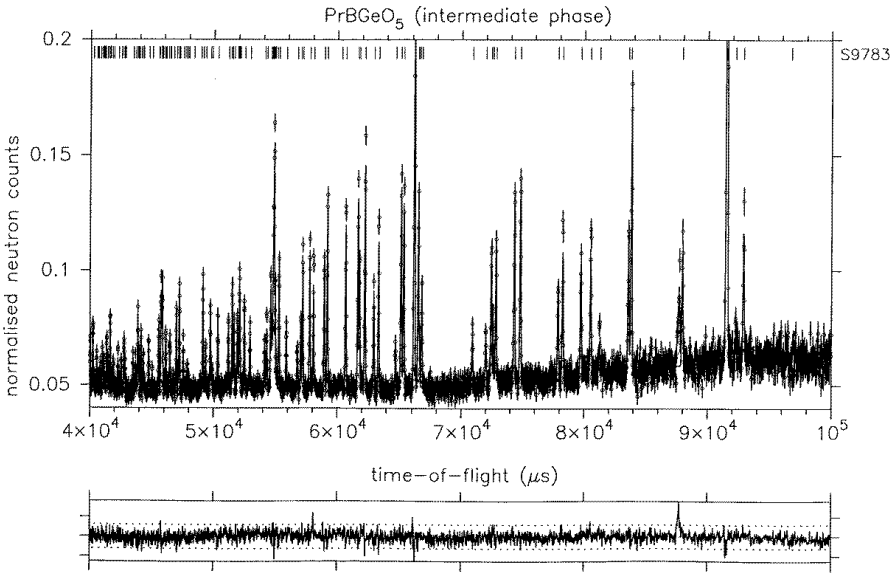

Figure 6. Powder profile refinements of $PrBGeO_5$ of the intermediate phase using data taken at 650 °C.

The Rietveld refinement of the structure of the high-temperature modification of $PrBGeO_5$ started from the structural parameters of $LaBGeO_5$ above its ferroelectric phase transition at 530 °C (high-temperature setting) and data from the long run measured at 800 °C. The best agreement (figure 7, table 5) was obtained with a split site for O(5), a tendency to splitting for O(3) (enlarged B_{ij}) and no splitting for the B atom. The resulting profile agreement factor was $R_{prof} = 4.89\%$, $R_{wprof} = 5.72\%$ and $\chi^2 = 2.168$ for 2325 observations. The structure closely resembles that of $LaBGeO_5$ at high temperature. The

absence of a split site for the B atom, in contrast to that found in $LaBGeO_5$, may be explained by the difference in the ionic radii of La and Pr leading to a simpler configuration in $PrBGeO_5$ of the double helical chain formed from Ge- and B-tetrahedra with normal interatomic distances (table 3).

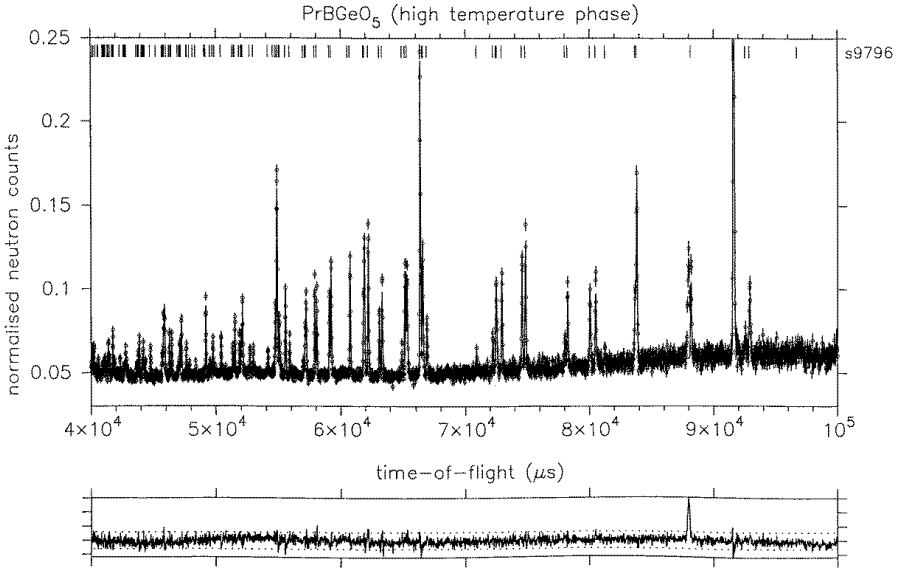

Figure 7. Powder profile refinements of $PrBGeO_5$ of the high-temperature phase using data taken at 800 °C.

Table 5. The positional and thermal parameters of the high-temperature phase of $PrBGeO_5$ as determined at 800 °C from neutron HRPD data.

Atom	*x*	*y*	*z*	B_{11}	B_{22}	B_{33}	B_{12}	B_{13}	B_{23}	Site occupancy
800 °C										
Pr	0.4098(2)	0	0.3333	1.59(9)						1
Ge	0.4231(5)	0	0.8333	1.31(6)						1
B	0.8902(8)	0	0.3333	1.46(9)						1
O(1)	0.1518(7)	0.5352(7)	0.0159(6)	1.86(8)						1
O(3)	0.1458(7)	0.6140(8)	0.3434(9)	2.8(2)	2.5(1)	2.9(2)	−0.4(2)	−0.2(2)	0.8(2)	1
O(5)	−0.0028(14)	0.0423(13)	0.7937(11)	1.7(1)						0.5

6. The first-order phase transition in $PrBGeO_5$ and its comparison with the second-order phase transitions in both $PrBGeO_5$ and $LaBGeO_5$ stillwellites

We are now able to discuss the mechanism for the first-order phase transition in $PrBGeO_5$ from its room temperature structure to the 'normal' $P3_1$ polar analogue of stillwellite. During this phase transition, one oxygen and one boron atom which break the smaller $\boldsymbol{a}$ translations must change positions from 'white' to 'black' leading to disappearance of the tripling. An analysis of the distances between the six possible positions for O(5) (figure 4(c))

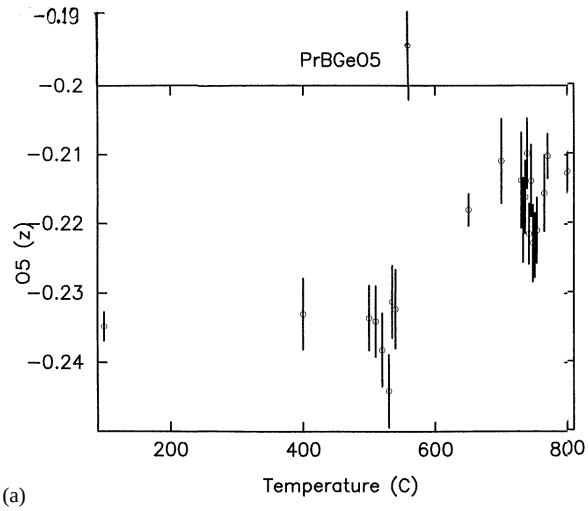

(a)

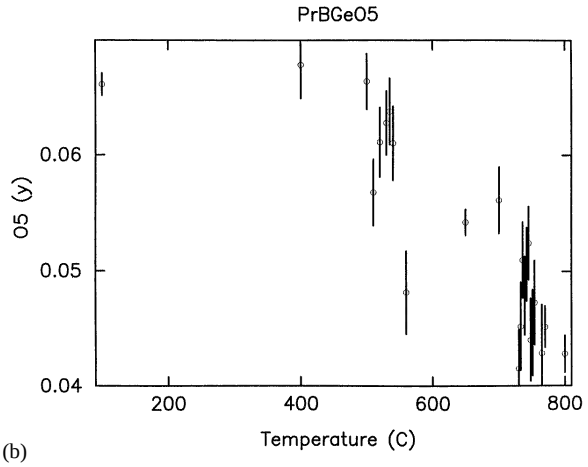

(b)

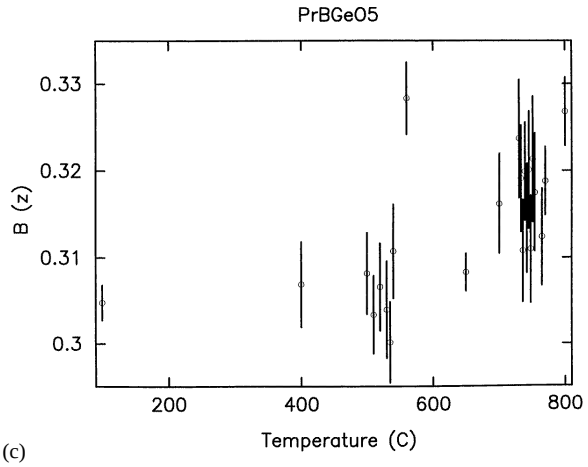

(c)

Figure 8. The thermal evolution of the atomic coordinates of the atoms (a) O(5) (z), (b) O(5) (y) and (c) B (z).

shows that there are two short distances of 1.33 and 1.218 Å, and the shortest jump is between 'black' and 'white' O(5)–O(5′) ∼1.2 Å. If some displacement of O(5) occurs closer to the phase transition which reduces the 1.218 Å distance, the jump will take place. It should be noted that oxygen atom jumps of ∼0.75 Å were found in the high-temperature, and of ∼0.7 Å in the high pressure, phase transition in $KTiOPO_4$ from neutron diffraction studies. Using the data sets collected for the unit cell refinements of the average small unit cell and applying the same procedure for refining the atomic coordinates as it was made in our study of $LaBGeO_5$ it is possible to follow the thermal evolution of the positional parameters of O(5) and B atoms. In the region of $T_c = 540\,^{\circ}$C, O(5) undergoes the largest displacement which is parallel to [001], but is also large along [010] and is clearly seen for the B atom along [001] (figure 8). The interatomic distances between the positions of the new 'black' and 'white' O(5) atoms at the extremal point gives a distance of ∼0.68 Å (figure 4(d)), which is suitable for a jump to occur. The 540 °C phase transition is of first order, discontinuous, and is characterized by the displacive jump of O(15) in the room temperature structure, which, in turn, removes the difference in orientation of all oxygen and boron atoms and removes tripling of the unit cell. It is accompanied by a discontinuity in the unit cell dimensions and its volume.

In contrast to the transition at 540 °C, the second phase transition at 742 °C is continuous second order in which a large displacement of O(5) over an extended range of temperature leads to a final position after which a jump of ∼0.746 Å occurs between O(5) and O(5′) followed by dynamic oscillations between these two positions (the order-disorder component of the transition) and the change of symmetry from $P3_1$ to $P3_121$.

7. Conclusion

The radius of the rare-earth cation is a very important factor in the structure type, which is stable only for La, Ce and Pr (see the introduction). La is the preferred element for the germanate analogue and it gives rise to good crystals, stable over a wide temperature range. In $LaBGeO_5$, the average La–O distance is 2.605 Å. In $PrBGeO_5$ the crystal structure of the stillwellite type is stable only between ∼540–∼742 °C because thermal expansion increases the average Pr–O distance from 2.558 Å at room temperature, where the structure is unstable and gives rise to twins, to 2.588 Å (close to the value in $LaBGeO_5$). The same effect as temperature is produced by isomorphous substitution of Pr by La: the region of stability of the normal polar modification is extended to lower temperatures. For $(Pr_{0.8}La_{0.2})BGeO_5$ the first phase transition typical for $PrBGeO_5$ disappears.

The results obtained in the investigation of the complex phase transitions enable us to explain the peculiarities of the non-linear optical properties of $PrBGeO_5$ (figure 2). The sharp increase in the intensity of the SGH signal is connected with an increase of polarity in the structure which is determined in the intermediate state by the O(5) and B atoms in the whole lattice, whereas in the room-temperature state only one out of three O(5) and boron atoms determines polarity. Pr, Ge and O(1–4) are also displaced in the phase transition and no longer possess the previous highly pseudo-symmetric positional coordinates as at room temperature (tables 2 and 4).

Analysis of the structural changes between the room-temperature and the intermediate-, and then between the intermediate- and the high-temperature modifications of $PrBGeO_5$ allows us to conclude that the transitions are significantly different in character. Whereas the former is of first order and displacive by nature, the latter is of second order with both displace and order-disorder elements as found in $LaBGeO_5$ [8]. We cannot exclude the presence of a small disordered component of the first phase transition if we assume

a short time oscillation between the O(15)–O(15′) positions. Specific heat measurements over the whole temperature interval from ambient to 800 °C, as were made for $LaBGeO_5$ [7] and recently for $LaBSiO_5$ [14], could show whether or not an order-disorder component exists in $PrBGeO_5$ since they would enable the entropy excess in the phase transition to be determined.

In the Si analogue $LaBSiO_5$ we also see dramatic effects produced by isomorphic substitution of larger Ge atoms by smaller Si: an increased pseudo-symmetry and a tilting of the chain [8] which influence the temperature at which the phase transition occurs and leads to a transition which is also of first order, but with an order-disorder component [14] and a very small displacement of O(5). Twinning is also typical for the ambient-temperature modification of $LaBSiO_5$.

The most remarkable feature of the high-temperature modification of all stillwellites is the existence of double helical chains of B tetrahedra in dynamic equilibrium, which results in the disappearance of the ferroelectric and non-linear optical properties. The higher Curie temperature in $PrBGeO_5$, $T_c = 742\,^{\circ}C$, in comparison with $LaBGeO_5$, $T_c = 530\,^{\circ}C$, is connected with the region of stability of $PrBGeO_5$ polar stillwellite-like modification being at a higher temperature. Thus, $PrBGeO_5$ may be recommended as a new material for application at high temperatures between 540 and 742 °C. We can expect that high pressure applied to $PrBGeO_5$ will displace this region of application to even higher temperatures.

Acknowledgments

The authors are very grateful to Dr B V Mill for giving us the single crystal material used in the investigation and to Dr S Yu Stefanovich for the physical measurements which led to the initial characterization of the two-phase transitions. ELB wishes to thank the Russian Foundation for Basic Research for its support under Project 96-02-17723a. We are especially thankful to the Royal Society whose financial support under its Joint Research Project 638072/P/737 enabled ELB to participate in the experimental measurements.

References

[1] Kaminskii A A, Mill B V, Belokoneva E L and Butasin A V 1990 *Izv. Akad. Nauk SSSR, Ser. Neorg. Mater.* **26** 1105
[2] Stefanovich C Yu, Mill B V and Butashin A V 1992 *Kristallografia* **37** 965
[3] Horiuchi N, Osakabe E, Uesu Y and Strukov B A 1995 *Ferroelectrics* **169** 273
[4] Kaminskii A A, Butashin A V, Maslyanizin J A, Mill B V, Mironov V S, Rozov S P, Sarkiskov S E and Shigorin V C 1991 *Phys. Status Solidi* a **125** 671
[5] Belokoneva E L, Mill B V, Butashin A V and Kaminskii A A 1991 *Izv. Akad. Nauk SSSR, Ser. Neorg. Mater.* **27** 556
[6] Uesu Y, Horinchi N, Osakobe E, Omori S and Strukov B A 1993 *J. Phys. Soc. Japan* **62** 2522
[7] Onodera A, Strukov B A, Belov A A and Taraskin S A 1993 *J. Phys. Soc. Japan* **62** 4311
[8] Belokoneva E L, David W I F, Forsyth J B and Knight K S 1997 *J. Phys.: Condens. Matter* **9** 3503
[9] Voronkov A and Pyatenko Yu A 1964 *Kristallografia* **12** 258
[10] Stefanovich S Yu, Mosunov A V, Mill B V and Butashin A V 1995 *Russ. J. Inorg. Chem.* **40** 867
[11] Stefanovich S Yu, Sigaev V N and Dechev A V 1994 *Int. Symp. Ferro-, Piezoelectric Materials and their Applications. (Abstr. Moscow PO-1-24)*
[12] Belokoneva E L, Shuvaeva V A and Antipin M Yu 1996 *Zh. Neorg. Chim.* **41** 1097
[13] Ono Y, Takayama K and Kajitani T 1996 *J. Phys. Soc. Japan* **65** 3224
[14] Strukov B A, Onodera A, Ragula E P, Stephanovich S Yu, Shnaidshtein I V and Archangelskaja S V 1998 *Fiz. Tverd. Tela* **40** 1310